solidation strategies after high-dose methotrexate-based chemoimmunotherapy in patients with primary CNS lymphoma: results of the second randomisation of the International Extranodal Lymphoma Study Group-32 phase 2 trial. Lancet Haematol 2017;4:e510-23.
6. Schorb E, Finke J, Ferreri AJ, et al. High-dose chemotherapy and autologous stem cell transplant compared with conventional chemotherapy for consolidation in newly diagnosed primary CNS lymphoma--a randomized phase III trial (MATRix). BMC Cancer 2016;16:282.
7. Grommes C, Pastore A, Palaskas N, et al. Ibrutinib unmasks critical role of bruton tyrosine kinase in primary CNS lymphoma. Cancer Discov 2017;7:1018-29.
8. Abramson JS, McGree B, Noyes S, et al. Anti-CD19 CAR T cells in CNS diffuse large-B-cell lymphoma. N Engl J Med 2017; 377:783-4.
9. Mendez JS, Ostrom QT, Gittleman H, et al. The elderly left behind-changes in survival trends of primary central nervous system lymphoma over the past 4 decades. Neuro Oncol 2018; 20:687-94.
10. Kasenda B, Ferreri AJ, Marturano E, et al. First-line treatment and outcome of elderly patients with primary central nervous system lymphoma (PCNSL)-a systematic review and individual patient data meta-analysis. Ann Oncol 2015;26:1305-13.
11. Fritsch K, Kasenda B, Schorb E, et al. High-dose methotrexate-based immuno-chemotherapy for elderly primary CNS lymphoma patients (PRIMAIN study). Leukemia 2017;31:846-52.
12. Abrey LE, Batchelor TT, Ferreri AJ, et al. Report of an international workshop to standardize baseline evaluation and response criteria for primary CNS lymphoma. J Clin Oncol 2005;23:5034-43.
13. Wang H, Wang M, Wei J, Wang L, Mao L, Jin J. Primary central nervous system lymphoma: Retrospective analysis of 34 cases in a single centre. J Int Med Res 2018;46:883-94.
14. Burton EC, Ugiliweneza B, Kolikonda MK, et al. A regional multicenter retrospective analysis of patients with primary central nervous system lymphoma diagnosed from 2000-2012: treatment patterns and clinical outcomes. Cureus 2017;9:e1512.

Acetate moderately attenuates the generation of neutrophil extracellular traps

TO THE EDITOR: It has been suggested that short-chain fatty acids (SCFAs) such as acetate, propionate, and butyrate, which are produced by the microbial fermentation of dietary fiber in the gut, exhibit several immunologic or metabolic effects. For example, SCFAs can modulate neutrophil migration [1, 2], induce the differentiation of regulatory T cells [3], and inhibit tumor necrosis factor-α production from macrophages [4, 5].

Recently, Vieira *et al.* [6] reported that treatment with acetate accelerated the resolution of inflammation in experimental mouse models of gout. The effects of acetate were shown to be mediated by accelerated neutrophil apoptosis, enhanced efferocytosis, reduced nuclear factor-κB activity, and an enhanced production of anti-inflammatory mediators including interleukin-10, transforming growth factor-β, and annexin A1.

Neutrophils exert their anti-microbial functions through the formation of neutrophil extracellular traps (NETs), the production of reactive oxygen species, and the secretion of several proteases such as elastase, lactoferrin, and lysozyme. NETs are composed of decondensed chromatin fibers coated with antimicrobial proteins such as myeloperoxidase, neutrophil elastase, and α-defensin [7]. However, NETs contribute to organ damage including acute lung injury, thrombosis formation, autoimmune pathologies, metastasis of malignant tumors, and atherosclerosis [7]. In this study, we investigated the effects of acetate on the formation of NETs.

The following methods were utilized. Heparinized peripheral blood was collected from healthy volunteers after obtaining their written informed consent. Neutrophil separation (>90% purity) was performed as reported previously [8]. This study was approved by the Ethics Committee of Himeji Dokkyo University (12-01, 17-08).

Phorbol myristate acetate (PMA), bovine serum albumin, nuclease from *Staphylococcus aureus*, ethylene glycol tetraacetic acid, diphenylene iodonium (DPI), and acetate were purchased from Sigma-Aldrich (St. Louis, MO, USA). SYTOX

Table 1. Lambda DNA was measured using SYTOX Green.

Acetate	Lambda DNA 0 ng/mL		1 ng/mL		3 ng/mL		5 ng/mL	
	Mean	SD	Mean	SD	Mean	SD	Mean	SD
0 mM	4,278	386	166,649	14,119	403,841	58,468	576,097	42,468
25 mM	4,344	445	164,181	14,809	419,319	51,839	576,772	68,383
50 mM	4,466	547	157,233	10,602	423,093	40,819	579,226	85,789

The linearity was unaffected by the addition of 25 or 50 mM acetate. No statistically significant difference was observed between the data with and without acetate addition (N=6).
Abbreviation: SD, standard deviation.

Green and SYTO 59 Red were obtained from Molecular Probes (Eugene, OR, USA).

Quantitative analysis was performed as described by Palmer *et al.* [9] with partial modification as reported previously [8]. Briefly, a 96-well plate was coated with 1% bovine serum albumin and 0.2 mL of purified neutrophils suspended in Roswell Park Memorial Institute 1640 medium was added to each well. The cells were stimulated with PMA for 3 hours at 37°C in humidified air with 5% CO_2 and acetate was simultaneously added. After nuclease treatment, the cells were transferred to Eppendorf tubes and centrifuged at 1,800× g for 10 min at 4°C. SYTOX Green, which is a nucleic acid stain that cannot permeate live cells, was added to the supernatants at a final concentration of 2.9 μM and fluorescence was detected at excitation and emission wavelengths of 488 and 520 nm, respectively. Relative fluorescence was then calculated by comparison with controls. The linearity of this method was confirmed again [8] and the addition of 25 or 50 mM acetate to this system did not alter the results (Table 1).

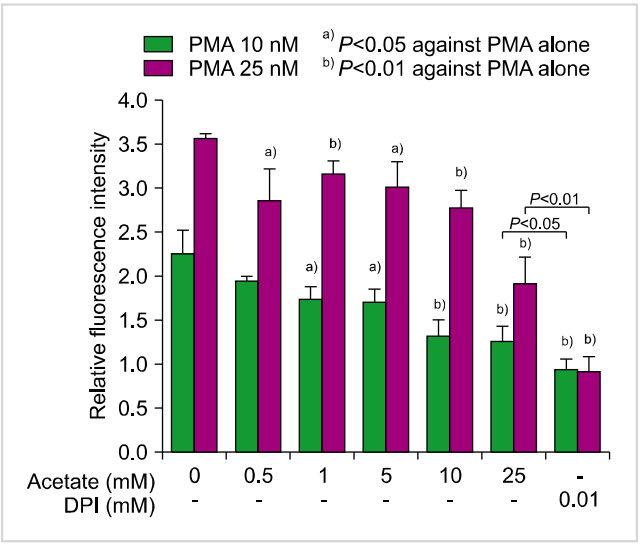

Fig. 1. Effects of short-chain fatty acids on NET generation and reactive oxygen species production. A quantitative analysis revealed that acetate had a dose-dependent inhibitory activity on NETs generation, although its potency was lower than that of DPI.

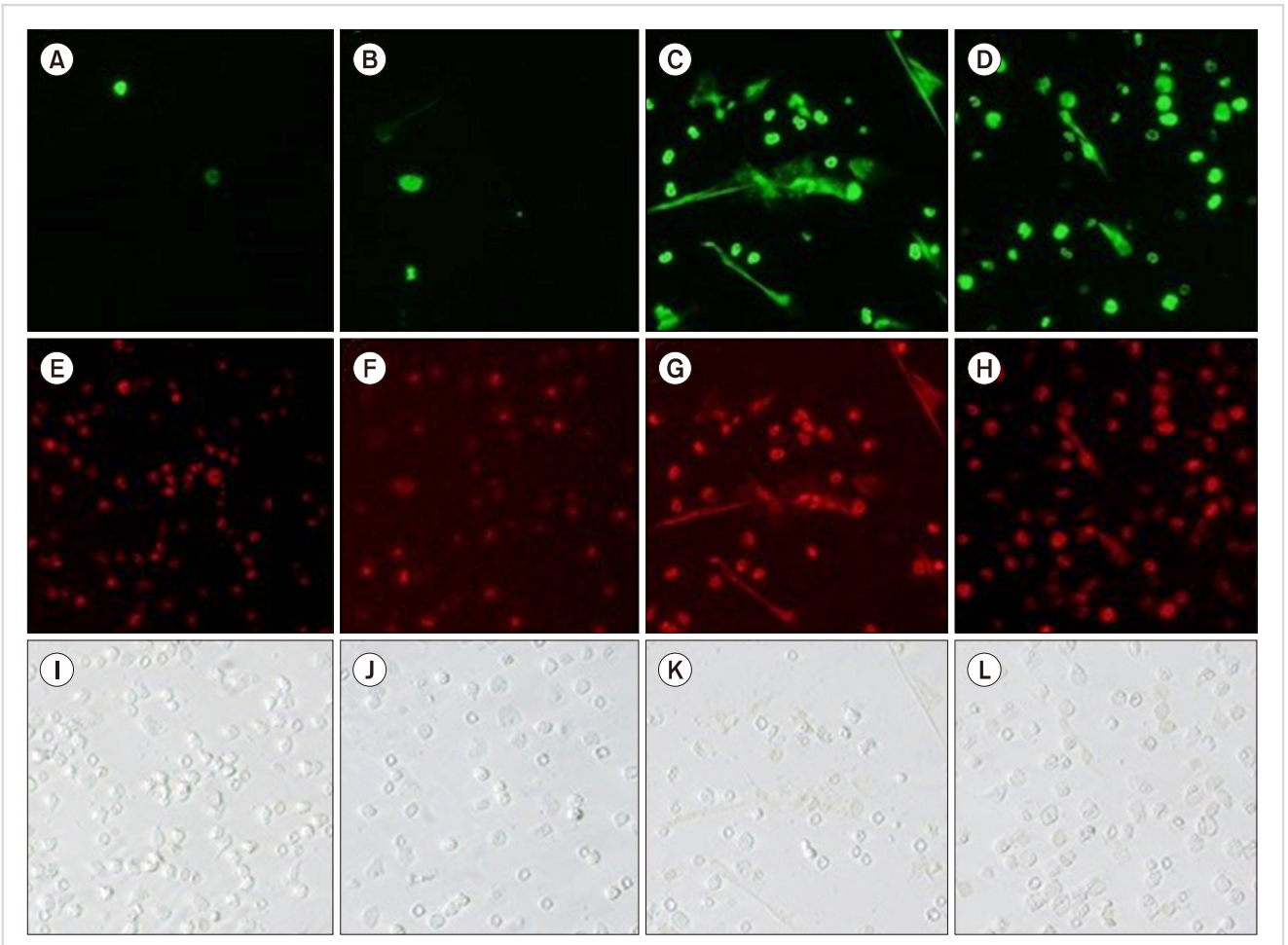

Fig. 2. Morphological observation by fluorescence microscopy. SYTOX Green staining revealed the ability of acetate to inhibit NETs. **(A, E, I)** Control; **(B, F, J)** 25 mM acetate alone; **(C, G, K)** 50 nM PMA alone; **(D, H, L)** 50 nM PMA with 25 mM acetate. (**A–D**, SYTOX Green staining) (**E–H**, SYTO 59 Red staining) (**I–L**, phase-contrast micrographs, ×100).

Table 2. Superoxide was detected using chemiluminescence.

PMA (nM)	0		16		32		
Acetate (mM)	0	25	0	25	0	25	-
DPI (mM)	-	-	-	-	-	-	0.01
Mean	3,250	3,305	30,106	29,550	37,149	35,545	6,681
SD	315	289	2,524	4,269	3,304	5,670	514
N	3	3	6	6	6	6	3
P	0.641		0.771		0.563		<0.01

Superoxide production induced by PMA was unaffected by 25 mM acetate.
Abbreviation: SD, standard deviation.

For morphological analysis, purified neutrophils were suspended in Hank's balanced salt solution with 5% heat-inactivated autologous serum at 1×10^9 cells/L. This cell suspension (250 μL) was then added to 35-mm glass-bottomed dishes coated with poly-L-lysine (Sigma-Aldrich) and incubated under the same conditions as those used for quantitative analysis. Next, SYTOX Green and SYTO 59 Red, which are both cell-permeable nucleic acid stains, were added at a concentration of 4 μM and stained neutrophils were observed under a fluorescence microscope (TH4-100 Cell Sens; Olympus, Tokyo, Japan) [8].

Superoxide production was detected by means of chemiluminescence with a device manufactured by Hamamatsu Photonics (Hamamatsu, Japan) as previously reported [10]. EZR (Easy R) was used for all statistical analyses [11], and paired *t*-tests were used to compare data from the two groups.

The following results were obtained. At concentrations exceeding 0.5 mM, acetate significantly inhibited PMA-induced NETs generation (Fig. 1, N=3–4) in a dose-dependent manner. However, the inhibition exerted by acetate was less potent than that exerted by DPI, which is a nicotinamide adenine dinucleotide phosphate (NADPH) oxidase inhibitor. A trypan blue dye exclusion test revealed that more than 98.5% of the cells were viable after 3 hours of incubation with 25 mM acetate. Fluorescence microscopic observation also revealed the inhibitory effect of acetate on PMA-induced NETs (Fig. 2). Micrographs are shown of the control (Fig. 2A), acetate treatment (25 mM) alone (Fig. 2B), the positive control treated with 50 nM PMA (Fig. 2C), and the combination of PMA and acetate (Fig. 2D). Figs. 2E–H show the corresponding SYTO 59 Red images of the corresponding areas and Figs. 2I–L show phase-contrast micrographs. These findings clearly indicate that treatment with 25 mM acetate attenuated PMA-induced NETs formation.

Since reactive oxygen species production is a prerequisite for PMA-induced NETs formation, the effects of acetate on superoxide formation were assessed by chemiluminescence. As shown in Table 2, acetate did not inhibit the induction of superoxide formation by either 8 or 16 nM PMA.

The concentration of acetate in the portal vein is reportedly 0.1–0.3 mM and that in the lumen of the colon is 20–140 mM [12]. In our experiments, low concentrations of acetate weakly inhibited PMA-induced NET formation, while higher concentrations similar to those available in the colonic lumen moderately inhibited NET formation, although the inhibitory effect of acetate was weaker than that of DPI. Considering these results, the biological significance of SCFAs in inflammatory bowel diseases (IBDs) is of interest. In the pathogenesis of IBDs such as ulcerative colitis and Crohn's disease, neutrophil activation is thought to result in tissue damage. NET production, in particular, has been shown to be involved in the thromboembolic events that are frequently observed in IBD patients [13]. Although pharmaceutical approaches for the control of IBDs have improved, a high proportion of patients remain refractory to current drugs. However, ongoing human studies have indicated that interventions with dietary fiber, which induces SCFAs generation through fermentation, show beneficial outcomes for IBDs [14]. The moderate inhibition of NETs generation by acetate as described here may be relevant to these clinical observations. Thus, studies are needed to determine the effects of combined treatments with acetate and other neutrophil-inhibitory substances such as antioxidants [15].

The effects of acetate are reportedly related to the G-protein-coupled receptor GPR43, which has been shown to be expressed on neutrophils [2]. Based on these findings, it is necessary to clarify the mechanism by which SCFAs can inhibit the activation of neutrophils.

Conclusion

NET formation is moderately inhibited by acetate through a currently unknown mechanism that is unrelated to NADPH oxidase inhibition.

Ayako Ohbuchi[1], Mari Kono[3], Mariko Takenokuchi[1], Shion Imoto[4], Katsuyasu Saigo[1,2]

[1]Faculty of Pharmacological Sciences, [2]Faculty of Nursing, Himeji Dokkyo University, Himeji, [3]Scientific Research Division, Scientific Affairs, Sysmex Corporation, Kobe, [4]Department of Health Science, Kobe Tokiwa University, Kobe, Japan

Correspondence to: Katsuyasu Saigo
Faculty of Nursing, Himeji Dokkyo University, 7-2-1 Kamiono, Himeji, Hyogo 670-8524, Japan

E-mail: ksaigo@himeji-du.ac.jp, saigok2@yahoo.co.jp

Received on Jan. 8, 2018; Revised on Apr. 13, 2018; Accepted on May 10, 2018

https://doi.org/10.5045/br.2018.53.2.177

Acknowledgments

This work was supported by JSPS Grant-in-Aid 15K08660 and Hyogo Medical Association Grant MRF-H-07-14 for K.S.

Authors' Disclosures of Potential Conflicts of Interest

No potential conflicts of interest relevant to this article were reported.

REFERENCES

1. Halnes I, Baines KJ, Berthon BS, MacDonald-Wicks LK, Gibson PG, Wood LG. Soluble fibre meal challenge reduces airway inflammation and expression of GPR43 and GPR41 in asthma. Nutrients 2017;9:E57.
2. Kamp ME, Shim R, Nicholls AJ, et al. G protein-coupled receptor 43 modulates neutrophil recruitment during acute inflammation. PLoS One 2016;11:e0163750.
3. Arpaia N, Campbell C, Fan X, et al. Metabolites produced by commensal bacteria promote peripheral regulatory T-cell generation. Nature 2013;504:451-5.
4. Vinolo MA, Rodrigues HG, Hatanaka E, Sato FT, Sampaio SC, Curi R. Suppressive effect of short-chain fatty acids on production of proinflammatory mediators by neutrophils. J Nutr Biochem 2011;22:849-55.
5. Nakajima A, Nakatani A, Hasegawa S, et al. The short chain fatty acid receptor GPR43 regulates inflammatory signals in adipose tissue M2-type macrophages. PLoS One 2017;12:e0179696.
6. Vieira AT, Galvão I, Macia LM, et al. Dietary fiber and the short-chain fatty acid acetate promote resolution of neutrophilic inflammation in a model of gout in mice. J Leukoc Biol 2017;101:275-84.
7. Kono M, Saigo K, Yamamoto S, et al. Iron-chelating agent, deferasirox, inhibits neutrophil activation and extracellular trap formation. Clin Exp Pharmacol Physiol 2016;43:915-20.
8. Ohbuchi A, Kono M, Kitagawa K, Takenokuchi M, Imoto S, Saigo K. Quantitative analysis of hemin-induced neutrophil extracellular trap formation and effects of hydrogen peroxide on this phenomenon. Biochem Biophys Rep 2017;11:147-53.
9. Palmer LJ, Damgaard C, Holmstrup P, Nielsen CH. Influence of complement on neutrophil extracellular trap release induced by bacteria. J Periodontal Res 2016;51:70-6.
10. Saigo K, Mori C, Iwamoto S, et al. Recombinant thrombomodulin does not impair neutrophil functions. J Thromb Thrombolysis 2015;39:536-8.
11. Kanda Y. Investigation of the freely available easy-to-use software 'EZR' for medical statistics. Bone Marrow Transplant 2013;48:452-8.
12. Ohira H, Tsutsui W, Fujioka Y. Are short chain fatty acids in gut microbiota defensive players for inflammation and atherosclerosis? J Atheroscler Thromb 2017;24:660-72.
13. Wéra O, Lancellotti P, Oury C. The dual role of neutrophils in inflammatory bowel diseases. J Clin Med 2016;5:E118.
14. Wong C, Harris PJ, Ferguson LR. Potential benefits of dietary fibre intervention in inflammatory bowel disease. Int J Mol Sci 2016;17:E919.
15. Al-Khafaji AB, Tohme S, Yazdani HO, Miller D, Huang H, Tsung A. Superoxide induces Neutrophil Extracellular Trap Formation in a TLR-4 and NOX-dependent mechanism. Mol Med 2016;22:621-31.

Granulocytic dysplasia: an indicator of clonal evolution in patients with chronic myeloid leukemia

TO THE EDITOR: A 38-year-old man with history of corrected rheumatic heart disease was incidentally diagnosed with *BCR-ABL1*-positive chronic myeloid leukemia (CML). He was treated with imatinib 400 mg/day, with which he achieved major molecular remission (MMR) after 12 months of therapy. He was followed up regularly with examinations of complete blood counts and 6-monthly quantitative *BCR-ABL1* transcript levels, which improved to MR4.5 in 24 months. After 4 years of regular treatment with good drug compliance, he showed loss of MMR on routine testing with increased *BCR-ABL1/ABL1* transcript levels of up to 32.4% on the international standard (IS) scale. Hemogram showed hemoglobin level of 68 g/L, leukocyte count of 4.6×10^9/L, and platelet count of 202×10^9/L. Peripheral blood film (PBF) showed leukoerythroblastic picture with eosinophilia (13%), basophilia (10%), and significant dysgranulopoiesis (Fig. 1A-C). Bone marrow was markedly hypercellular with 4% blasts, marked dysgranulopoiesis, dysmegakaryopoiesis (>90% dwarf forms) (Fig. 1D, E), eosinophilia (16%), and basophilia (9%). This morphology was consistent with a loss of hematological responses. Conventional cytogenetics revealed 49,XY,+8,t(9;22)(q34;q11.2),i(17)(q10),+der(22)t(9;22)(q34;q11.2). Fluorescent in situ hybridization (FISH) using the Vysis *BCR/ABL1/ASS1* Tri-Color Dual Fusion Probe and *TP53*/CEP17 dual colour Probe (Abbott Molecular, Abbot Park, IL, USA) confirmed the presence of an additional Philadelphia chromosome and loss of one copy of *TP53* gene in concordance with isochromosome 17q (Fig. 1F, G). In a patient who previously achieved MMR, these cytogenetic abnormalities suggest clonal evolution and hence are consistent with accelerated phase of CML. In view of secondary resistance to imatinib therapy, *ABL* kinase domain mutation analysis by Sanger sequencing was performed, which did not reveal any mutations. He was subsequently administered dasatinib 100 mg daily. However, after 2 weeks of treatment, the patient developed symptoms of fluid overload and heart failure attributed to dasatinib. The dose of dasatinib was then decreased to 50 mg daily, which was well tolerated. The patient showed normalization